Eur. Phys. J. B **9**, 105–115 (1999)

THE EUROPEAN PHYSICAL JOURNAL B

EDP Sciences

Surface flows of granular mixtures

III. Canonical model

T. Boutreux[1,a], H.A. Makse[1,2,b], and P.-G. de Gennes[1]

[1] Laboratoire de Physique de la Matière Condensée[c], Collège de France, 11 place Marcelin Berthelot, 75231 Paris Cedex 05, France
[2] Center for Polymer Studies and Physics Department, Boston University, Boston, Massachusetts 02215, USA

Received 9 September 1998 and Received in final form 4 November 1998

Abstract. We present the generalization of the minimal model for surface flows of granular mixtures, proposed by Boutreux and de Gennes [J. Phys. I France **6**, 1295 (1996)]. The minimal model was valid for grains differing only in their surface properties. The present model also takes into account differences in the size of the grains. We apply the model to study segregation in two-dimensional silos of mixtures of grains differing in size and/or surface properties. When the difference in size is small, the model predicts that a continuous segregation appears in the static phase during the filling of a silo. When the difference in size is wide, we take into account the segregation of the grains in the rolling phase, and the model predicts complete segregation and stratification in agreement with experimental observations.

PACS. 83.70.Fn Granular solids – 83.10.Pp Particle dynamics – 47.55.Kf Multiphase and particle-laden flows

1 Introduction

Segregation of mixtures of grains is commonly observed in granular materials that are poured, vibrated, or rotated [1–19]. This phenomenon has great importance in industrial processes. The simplest way to observe segregation is to pour a mixture of grains of different sizes onto a heap; one obtains a heap with the large grains near the bottom and the small grains near the top [20–25].

The mixture can also be poured in a two-dimensional silo made up of two vertical plates separated by a gap of approximately 5 mm (a granular Hele-Shaw cell), as studied recently by Makse *et al.* [26–29]. Different forms of segregation are observed when the grains differ both in their size and their surface properties (shape, roughness, stickiness). When the grains do not differ much in size, the larger or the smoother grains stop preferentially at the bottom of the slope, and the smaller or the rougher at the top of the slope. This segregation is limited since grains of both species remain present everywhere; this phenomenon is called *continuous segregation*.

When the grains have a wide difference in size, segregation is stronger and appears in two different ways. When the large grains are smoother than the small ones, a *complete* segregation is observed, where all large grains stop near the bottom of the slope, and all small grains stop near the top. When the large grains are rougher than the small grains, a spectacular *stratification* is obtained, where the grains deposit in alternating layers of different species, parallel to the sandpile surface.

Theoretical studies of surface flows of grains were triggered by the works of Bouchaud, Cates, R. Prakash, and Edwards (BCRE) [30,31] and Mehta and collaborators [32]. BCRE proposed a set of coupled equations to describe granular flows in one species sandpiles. Boutreux and de Gennes (BdG) [33,34] generalized the BCRE equations in order to describe granular mixtures composed of two species. They proposed a theoretical formalism, and a *minimal* model describing the case of grains with different surface properties but equal size. In this case, BdG found a power law behavior of the concentrations which explains the continuous segregation. Since the minimal model does not take into account the size difference between the grains, Boutreux has treated the important case where the grains differ only in size, in a second article [35, 36] of the series started by BdG [34].

In the present article, the third and last one of the series, we treat the general case of the canonical model, by describing different examples where the grains differ in size and/or surface properties. We first assume that the two species do not differ much in size. We then consider that there is no segregation inside the rolling phase, which is homogeneous in the vertical direction. In this case,

[a] e-mail: `boutreux.thomas@bcg.com`
[b] e-mail: `makse@ridgefield.sdr.slb.com`.
Present address: Schlumberger-Doll Research Ridgefield, Connecticut 06877 USA.
[c] CNRS – URA 792

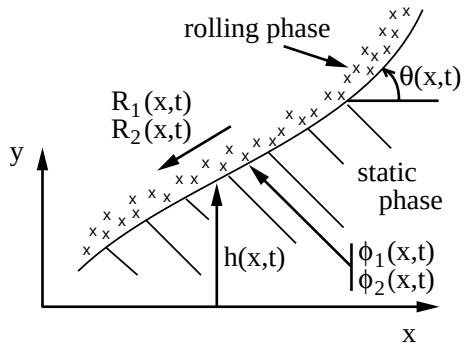

Fig. 1. Diagram showing the variables used to describe the granular flow of mixtures in a two-dimensional silo.

we show that the canonical model predicts continuous segregation (in agreement with experiments) with a power law behavior of the concentrations.

In the last part of the article, we consider the case in which the two species have a wide difference in size. We argue that in this case segregation probably occurs directly inside the rolling phase; due to percolation of the small grains, the small grains fall through the gaps between the large ones. We show that by taking this phenomenon into account and relaxing the assumption that the rolling phase is homogeneous, complete segregation occurs when the small grains are rougher than the large grains, and stratification occurs when the large grains are rougher than the small grains, in agreement with experiments. In these cases, our results are consistent with theoretical studies recently published by Makse, Cizeau, and Stanley (MCS) [37–39], who proposed a modified version of the BdG equations. MCS proposed a model valid for a mixture of grains with very different size. They explained the complete segregation phenomenon by predicting an exponential behavior of the concentrations, and successfully reproduced the mechanism leading to stratification as observed in the experiments.

The present article is organized as follows. In Section 2, we review the theoretical formalism developed in [30–34]. In Section 3, we present our model of binary collisions between one rolling grain and one grain at rest, and we obtain the canonical model for surface flows of granular mixtures. Section 4 describes the application of the model to all possible cases, when the two granular species differ in size and/or in surface properties. Then in Section 5, we model the steady state filling of a two-dimensional silo by a mixture of grains, and we discuss the predicted segregation profiles according to the different composition of the mixture. Finally in Section 6, we consider the case in which the grains have a wide difference in size, in order to describe stratification and complete segregation.

2 Theoretical formalism

The study of two-dimensional surface flows of granular materials has progressed significantly with the works of BCRE [30,31] and Mehta *et al.* [32]. BCRE proposed a set of variables and a set of coupled equations to describe two-dimensional granular flows for a pure species of grains. Recently, BdG [34] generalized the BCRE formalism by considering a mixture of two granular species. In the present paper, we describe this formalism for two species. Following Bouchaud *et al.*, we assume that there is a sharp distinction between a static phase, where grains at rest belong to the pile, and a thin rolling phase where grains are not part of the pile but roll downwards on top of the static phase (see Fig. 1). We call $\theta(x,t)$ the local slope of the interface, and $h(x,t)$ the height of the static phase. These quantities are to be understood as an average over a certain coarse grain length on the surface of the sandpile (larger than the size of the grains), where hydrodynamic equations are valid. For notational convenience we do not consider the difference between the angle θ and its tangent

$$\theta(x,t) \simeq -\frac{\partial h}{\partial x}\cdot \tag{1}$$

We call $\phi_\alpha(x,t)$ the volume fractions of the two species of grains in the static phase just below the interface (here the index α denotes the grain species, and is equal to "1" or "2"). We have $\phi_1 + \phi_2 = 1$. We assume that both species have a small difference in size, so that there is no segregation inside the rolling phase, *i.e.*, the rolling phase is homogeneous in the vertical direction (this assumption will be released in Sect. 6). We call $R(x,t)$ the total thickness of the rolling phase. We also consider two "equivalent thicknesses" for the two species in the rolling phase $R_\alpha(x,t)$ (*i.e.*, the total thickness multiplied by the local volume fraction of the α grains in the rolling phase at position x). The total thickness of the rolling phase is then equal to

$$R(x,t) \equiv R_1(x,t) + R_2(x,t). \tag{2}$$

The equations describing surface flow of grains take into account the fact that grains in the rolling phase move downwards due to their weight, and collisions between the rolling grains and the static grains induce exchanges between the two phases. The equation that describes the exchange of grains between the two phases is

$$\dot{h} = -(\dot{R}_1|_{coll} + \dot{R}_2|_{coll}), \tag{3}$$

where the dot denotes a time derivative, and $\dot{R}_\alpha|_{coll}$ the exchange between the α grains in the rolling phase with the static phase. Equation (3) can also be written for the single species

$$\phi_\alpha \dot{h} = -\dot{R}_\alpha|_{coll}. \tag{4}$$

The evolution equation for each species in the rolling phase, taking into account the downhill convection of grains due to gravity, is

$$\dot{R}_\alpha = v\frac{\partial R_\alpha}{\partial x} + \dot{R}_\alpha|_{coll}, \tag{5}$$

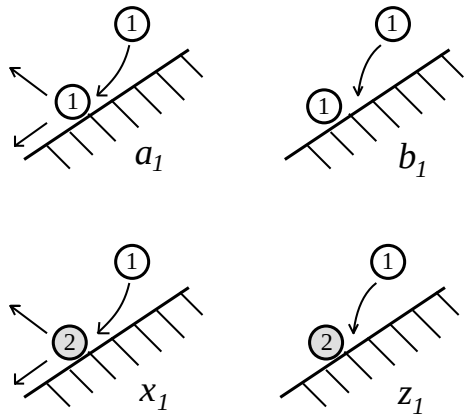

Fig. 2. Diagram showing the different type of collisions between a rolling grain of type 1, and a static grains of type 1 or 2. a_1: auto-amplification, x_1: cross-amplification, b_1: auto-capture, z_1: cross-capture.

where v is the convection speed of the rolling grains, which may depend on the slope $\theta(x,t)$ and on the grain species. However, we assume that the two species are mixed inside the rolling phase; the convection speed v must be identical for the two species. Moreover, in practice variations in the angle θ are small enough, so that the speed v can then be taken as a constant.

3 Canonical model

We propose a microscopic model of the grain collisions, that will allow us to calculate the exchange term $\dot{R}_\alpha|_{coll}$ as a function of θ, R_α, and ϕ_α. We calculate, in first order approximation, the interaction term $\dot{R}_\alpha|_{coll}$ by considering the binary collisions between one rolling grain and one grain at rest on top of the static phase. Collisions between three grains (or more) are less probable, and will be neglected. We consider four types of collisions for a rolling grain of type 1 (Fig. 2):

– Auto-amplification: another type 1 grain starts to roll. This collision contributes with a term $a_1(\theta)\phi_1 R_1$ to $\dot{R}_1|_{coll}$. This term is proportional to R_1 because all type 1 rolling grains interact with the static phase due to the fact that the rolling phase is thin. It is also proportional to the concentration of type 1 grains in the static phase, ϕ_1. The function $a_1(\theta)$ is called the *collision function* for the auto-amplification of type 1 grains. This function is positive, has dimensions of a frequency, and depends *a priori* on the angle θ. The collision functions may also depend on the type of species in the static phase that are in contact with the grain about to roll; the rougher the neighboring grains, the less chance for the static grain to start rolling, and the smaller the value of a_1. However, this neighbouring effect is expected to be small compared to the variations of a_1 with respect to θ. In order to simplify, we will neglect the neighbouring effect, and will consider that a_1 only depends on θ. The same approximation will be used for all the other collision functions.
– Cross-amplification: a type 2 grain starts to move. This collision contributes with a term $x_1(\theta)\phi_2 R_1$ to $\dot{R}_2|_{coll}$.
– Auto-capture: the type 1 rolling grain is captured after a collision with a type 1 static grain. This process contributes with a term $-b_1(\theta)\phi_1 R_1$ to $\dot{R}_1|_{coll}$.
– Cross-capture: the type 1 rolling grain is captured by a type 2 static grain. This process contributes with a term $-z_1(\theta)\phi_2 R_1$ to $\dot{R}_1|_{coll}$. This cross-capture interaction was not taken into account in the minimal model [34]. It plays an important role when the grains have different sizes, as will appear later.

Collisions where the rolling grain stops and simultaneously a static grain starts to roll are a limiting case between cross-amplification and cross-capture. The probability that these two collisions happen simultaneously is low, and therefore we neglect this process.

When the colliding rolling grain belongs to the type 2 species, four similar binary collisions occur. We call the corresponding collision functions $a_2(\theta)$, $x_2(\theta)$, $b_2(\theta)$, and $z_2(\theta)$, which are all positive. Since increasing the slope of the pile favors rolling, the amplification functions a_α and x_α are increasing functions of θ. Conversely, since decreasing the slope favors capture, the capture functions b_α and z_α are decreasing functions of θ.

It is now possible to write the expressions of the exchange term $\dot{R}_\alpha|_{coll}$ in a matrix form. We define the *collision matrix* $\hat{M}$ by [34]

$$\begin{pmatrix} \dot{R}_1|_{coll} \\ \dot{R}_2|_{coll} \end{pmatrix} = \hat{M} \cdot \begin{pmatrix} R_1 \\ R_2 \end{pmatrix}. \tag{6}$$

The previous microscopic description yields

$$\hat{M} = \begin{pmatrix} (a_1 - b_1)\phi_1 - z_1\phi_2 & x_2\phi_1 \\ x_1\phi_2 & (a_2 - b_2)\phi_2 - z_2\phi_1 \end{pmatrix}. \tag{7}$$

The elements $\mathrm{M}_{\alpha\beta}$ are determined by the concentrations $\phi_\alpha(x,t)$, and by the local angle $\theta(x,t)$ *via* the collision functions.

Next we calculate the expressions of the collision functions by doing a linear approximation around the angles of repose. In order to do so, let us consider the quantity E_1 defined as the total exchange (including capture and amplification) between the static phase and the rolling phase due to collisions originated by type 1 rolling grains – similar definition can be provided for the type 2 rolling grains, E_2. A type 1 rolling grain can interact – *via* auto-amplification or auto-capture – with other type 1 static grains giving rise to a contribution $(a_1 - b_1)\phi_1 R_1$ to E_1, or it can interact – *via* cross-amplification or cross-capture – with type 2 static grains giving rise to a contribution $(x_1 - z_1)\phi_2 R_1$ to E_1. Then E_1 is given by

$$\begin{aligned} E_1 &= [(a_1 - b_1)\phi_1 + (x_1 - z_1)\phi_2]R_1 \\ &= (M_{11} + M_{21})R_1. \end{aligned} \tag{8}$$

Notice that E_1 contributes to $\dot{R}_1|_{coll}$ *via* M_{11}, and also to $\dot{R}_2|_{coll}$ *via* M_{21}.

In a model of a single species made of type 1 grains, the exchange term would be equal to $E_1 = [a_1(\theta) - b_1(\theta)]R_1(x,t)$, and the angle θ for which $a_1 = b_1$ would correspond to the situation where there is no exchange of grains between the static and the rolling phases. We call this angle the *angle of repose* of the pure type 1 grains, which we denote θ_{11}, and it is the maximum angle below which a rolling grain is converted into a static grain. In general, the repose angle $\theta_{\alpha\alpha}$ of the pure α species is the angle at which the auto-amplification and auto-capture functions intersect

$$a_\alpha(\theta_{\alpha\alpha}) = b_\alpha(\theta_{\alpha\alpha}). \tag{9}$$

Moreover, we will call the *cross-angle of repose* $\theta_{\alpha\beta}$ the angle for which the cross-amplification function equals the cross-capture function

$$x_\alpha(\theta_{\alpha\beta}) = z_\alpha(\theta_{\alpha\beta}). \tag{10}$$

The angle θ_{12} for the type 1 grains is defined by $x_1(\theta_{12}) = z_1(\theta_{12})$, and corresponds to the angle of repose of a single type 1 rolling grain moving on top of a surface made exclusively of type 2 static grains [37]. One way to measure experimentally the cross-angles of repose would be by gluing grains of one species to an inclined plane and pouring grains of the other species and measure the angle at which grains stop to roll.

When the surface properties of the two species are not very different, the two pure angles of repose do not differ very much. Moreover, when the size of the grains do not differ much, the cross-angle of repose are also close. In practice, the angle θ remains close to the angles of repose of the species and we can linearize the eight collision functions with respect to θ to get a simple expression for E_1

$$E_1 = [\gamma_1(\theta - \theta_{11})\phi_1 + \gamma_2(\theta - \theta_{12})\phi_2]R_1, \tag{11}$$

where

$$\gamma_1 \equiv \partial_\theta a_1 - \partial_\theta b_1, \qquad \gamma_2 \equiv \partial_\theta x_1 - \partial_\theta z_1. \tag{12}$$

In order to consider the simplest case, we assume that all the derivatives of the collision functions have the same order of magnitude, *i.e.*

$$\partial_\theta a_1 \simeq \partial_\theta x_1 \simeq -\partial_\theta b_1 \simeq -\partial_\theta z_1, \tag{13}$$

so that $\gamma_1 \simeq \gamma_2 \equiv \gamma$, and therefore

$$E_1 = \gamma[\theta - \theta_1(\phi_2)]R_1, \tag{14}$$

where the angle $\theta_1(\phi_2)$ is given by

$$\theta_1(\phi_2) \equiv \theta_{11} + (\theta_{12} - \theta_{11})\phi_2. \tag{15}$$

The constant γ has the dimensions of frequency, and has typical value $\gamma \sim 25\ \mathrm{s}^{-1}$ [27]. Dimensional analysis show that the order of magnitude of γ is given by

$$\gamma \simeq v/d, \tag{16}$$

where d is the typical size of the grain. The constant γ represents the frequency of interaction between a rolling grain and the static phase. The larger the value of γ, the more frequent the exchange between phases.

Equation (14) shows that $\theta_1(\phi_2)$ is a cross-over angle; E_1 describes capture of rolling grains ($E_1 < 0$) when $\theta < \theta_1$, and amplification of grains ($E_1 > 0$) when $\theta > \theta_1$. The angle $\theta_1(\phi_2)$ for a mixture of grains plays the role of the constant angle of repose θ_{11} for a pure species of grains; the angle $\theta_1(\phi_2)$ is called the *generalized angle of repose* for the type 1 species. When no type 2 grains are present on the static phase ($\phi_2 = 0$), $\theta_1(\phi_2)$ (given by Eq. (15)) is equal to the angle of repose θ_{11} of the pure type 1 species. When ϕ_2 increases, the type 1 rolling grains interact more frequently with type 2 static grains, and the generalized angle of repose $\theta_1(\phi_2)$ changes.

The generalized angle of repose was introduced by MCS [37], who have shown that it has a key role in explaining the segregation as well as the stratification of granular mixtures. MCS defined the generalized angle of repose $\theta_\alpha(\phi_\beta)$ of species α as a linear function of the volume fraction ϕ_β and proposed the expression (15). In the present paper we show that this expression can be derived, by using the binary collision model and a linear development approximation. When it is possible, notations of reference [37] are used in the present paper.

Making similar approximations, we get a simplified expression for the exchange E_2 due to collisions with type 2 rolling grains

$$E_2 = \gamma[\theta - \theta_2(\phi_2)]R_2, \tag{17}$$

where

$$\theta_2(\phi_1) \equiv \theta_{22} + (\theta_{21} - \theta_{22})\phi_1 \tag{18}$$

is the generalized angle of repose for the type 2 species.

The generalized angles of repose quantify the degree of interaction of the rolling species with the pile. If the species α have a smaller generalized angle of repose for any value of ϕ_α, then, when $R_1 = R_2$, the α rolling grains are less captured (or amplify more grains in the bulk), than the other species. In order to quantify this behavior, we define the difference

$$\psi_{12} \equiv \theta_1(\phi_2) - \theta_2(\phi_1). \tag{19}$$

In the general case, ψ_{12} is a function of ϕ_α. However in order to simplify, in the following we will consider particular situations where ψ_{12} is a constant that does not depend on ϕ_α (*i.e.* $\theta_{12} - \theta_{11} = \theta_{22} - \theta_{21}$).

It is now possible to write a simpler expression for the collision matrix (7). Previous calculations for E_α yield

$$\hat{M} = \begin{pmatrix} \gamma[\theta - \theta_1(\phi_2)] - x_1(\theta)\phi_2 & x_2(\theta)\phi_1 \\ x_1(\theta)\phi_2 & \gamma[\theta - \theta_2(\phi_1)] - x_2(\theta)\phi_1 \end{pmatrix}, \tag{20}$$

where the cross-amplification functions can be written in the following way

$$x_1(\theta) = \frac{\gamma}{2}(\theta - \theta_{11}) + x_0, \qquad x_2(\theta) = x_1(\theta) - \Delta x_{12}. \tag{21}$$

Here x_0 and Δx_{12} are two constants of the model. We call equations (20) and (21) the canonical form of the collision matrix. This canonical form is general, and valid for any mixture of two granular species. In practice, the grains differ in size and in surface properties. Let us now see how the canonical form of the collision matrix conveys these differences.

4 Possible differences between the granular species

4.1 Grains differing only in their size

Let us consider the case where we mix species of small grains, denoted the $'s'$ species, with species of large grains, denoted the $'l'$ species, both species having similar densities and the same shape or roughness (in this case, indices $'1'$ and $'2'$ are replaced by indices $'s'$ and $'l'$). The size difference between the two species allows us to compare the collision functions. A large grain more easily sets a small grain into motion than the reverse, hence

$$x_s(\theta) < x_l(\theta). \tag{22}$$

A small grain is more easily captured on a surface of large grains than the reverse, then

$$z_l(\theta) < z_s(\theta). \tag{23}$$

Equations (22, 23) imply that the two cross-angles $\theta_{\alpha\beta}$, defined by equation (10), satisfy

$$\theta_{ls} < \theta_{sl}. \tag{24}$$

The size difference between the two species does not allow a comparison to be made between either the functions $a_l(\theta)$ and $a_s(\theta)$ or between the functions $b_l(\theta)$ and $b_s(\theta)$.

However considering that the $'l'$ and $'s'$ species have the same surface properties, we can obtain other inequalities. In first order approximation, the probability that an $'s'$ static grain is set into motion by an $'s'$ rolling grain is equal to the probability that an $'l'$ static grain is set into motion when it is collided by an $'l'$ rolling grain. The two probabilities are approximately equal because in both collisions the two interacting grains have the same weight, and because the two interacting surfaces are identical. Hence we have

$$a_s \simeq a_l \equiv a. \tag{25}$$

Similarly, the probability that a rolling grain is captured by a static grain belonging to the same species does not depend on the grain species being $'s'$ or $'l'$, then

$$b_s \simeq b_l \equiv b. \tag{26}$$

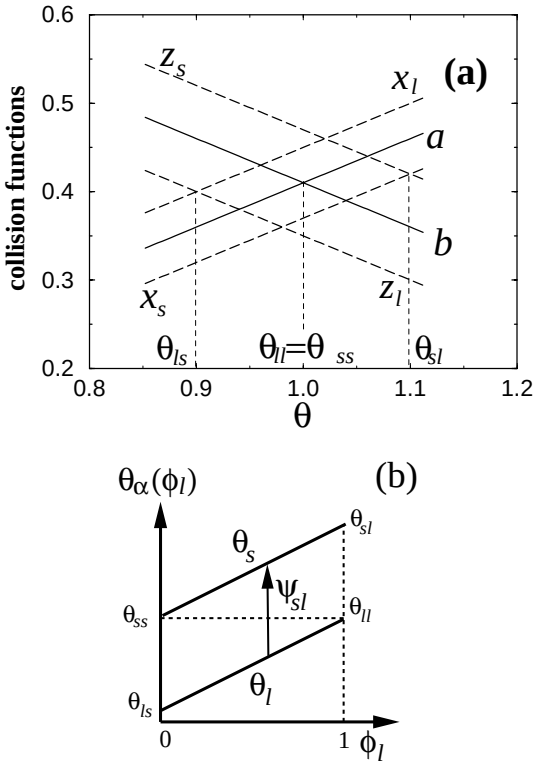

Fig. 3. Case A: grains differing only in their sizes (small type s and large type l grains). (a) Diagram of the collision functions. (b) Diagram of the generalized angles of repose as a function of the volume fraction ϕ_l. The angles of repose θ_{ss} and θ_{ll} for the two pure species are equal. Due to the size difference, the cross-angles of repose θ_{ls} and θ_{sl} are different.

Equations (25, 26) imply that the two pure angles $\theta_{\alpha\alpha}$ (defined by Eq. (9)) satisfy

$$\theta_{ll} = \theta_{ss}. \tag{27}$$

Thus, the present model shows that two granular species with identical surface properties have also identical angles of repose, as observed in experiments. Finally, the size difference between the two species involved in collisions yields

$$x_s < a < x_l, \qquad z_l < b < z_s. \tag{28}$$

We consider the simplest case by using the set of simplest relations consistent with equations (28)

$$a = (x_s + x_l)/2, \qquad b = (z_s + z_l)/2. \tag{29}$$

Equations (28) imply the following relations for the angles of repose, as proposed by MCS [37]

$$\theta_{ls} < \theta_{ll} = \theta_{ss} < \theta_{sl}. \tag{30}$$

The collision functions and the generalized angles of repose $\theta_l(\phi_s)$ and $\theta_s(\phi_l)$ arerepresented in Figures 3a and 3b.

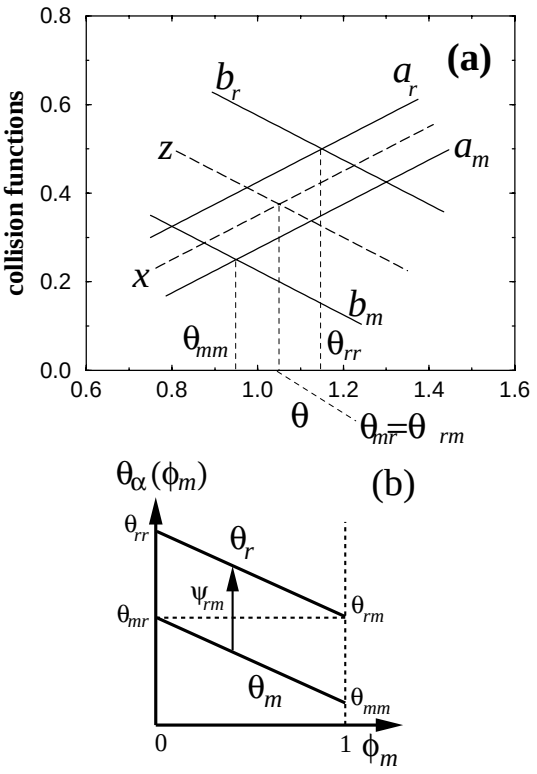

Fig. 4. Case B: grains differing only in their surface properties (rough type r and smooth type m grains). (a) Collision functions. (b) Generalized angles of repose: due to the surface differences the two angles of repose θ_{ss} and θ_{ll} of the pure species are now different, but the cross-angles of repose are the same due to the equal size of the grains.

Note that due to our assumptions (29), $\psi_{sl} \equiv \theta_s(\phi_l) - \theta_l(\phi_s)$ is a constant independent of ϕ_α. The angles of repose θ_{ss} and θ_{ll} of both pure species are equal due to their equal shapes, but due to the size difference between the particles we have $\psi_{sl} > 0$ for any value of ϕ_α; the l rolling species amplifies more easily the rolling phase than the s rolling species, because large grains are less easily captured, and more easily set another grain into motion. The larger the size difference between the two species, the larger the value of ψ_{sl} and the larger the strength of the exchange processes. In our case, ψ_{sl} is a small constant so that the linear development of the collision functions remains valid.

4.2 Grains differing only in their surfaces properties

Let us now consider the case where we mix species of rough grains, denoted the $'r'$ species, with species of smooth grains, denoted the $'m'$ species. The rougher the surface of a grain species, the more efficient a collision between two grains belonging to this species. Hence we have

$$a_m(\theta) < a_r(\theta), \qquad b_m(\theta) < b_r(\theta). \tag{31}$$

Experiments show that granular species with the smoother surface have also the smaller angle of repose: $\theta_{mm} < \theta_{rr}$ [27]. This inequality is equivalent to the condition

$$a_r - a_m < b_r - b_m. \tag{32}$$

Thus the last inequality is an experimental constraint for our model.

The different surface properties between the two species does not allow a comparison to be made between either the functions x_m and x_r or between the functions z_m and z_r. However, if we also assume that the $'r'$ and $'m'$ species have the same size, both cross-interactions correspond to collisions where two grains of the same mass interact *via* a rough surface in contact with a smooth surface. In first order approximation, the probability of a cross-interaction does not change if the two grains involved in the collision are switched, hence

$$x_r \simeq x_m \equiv x, \qquad z_r \simeq z_m \equiv z. \tag{33}$$

Equations (33) imply

$$\theta_{rm} = \theta_{mr}. \tag{34}$$

Finally, the surface differences between the two species involved in collisions yield

$$a_m < x < a_r, \qquad b_m < z < b_r. \tag{35}$$

We take the simplest relations consistent with equations (35)

$$x = (a_m + a_r)/2, \qquad z = (b_m + b_r)/2. \tag{36}$$

Equations (35) imply the following relations for the angles

$$\theta_{mm} < \theta_{rm} = \theta_{mr} < \theta_{rr}. \tag{37}$$

The collision functions and the generalized angles of repose $\theta_r(\phi_m)$ and $\theta_m(\phi_r)$ are shown in Figures 4a and 4b. Here again ψ_{rm} is a small constant due to our assumptions (36) and due to the validity of the linear approximations. Since m rolling grains are less easily captured, they amplify more easily the rolling phase than the r rolling grains.

4.3 Mixture of small rough grains and large smooth grains

We denote "type 1" grains the small rough grains, and "type 2" the large smooth grains (here we have $1 = s = r$, and $2 = l = m$). The size difference between the two species still yields equations (22) and (23), and the cross-angles of repose verify $\theta_{21} < \theta_{12}$. Moreover, the surface differences still imply equations (31), and the angles of repose verify $\theta_{22} < \theta_{11}$. If the size difference is very small, effects due to the surface differences are stronger, and we get $\theta_{22} < \theta_{21} < \theta_{12} < \theta_{11}$. This case is close to the situation where grains differ only in their surface properties.

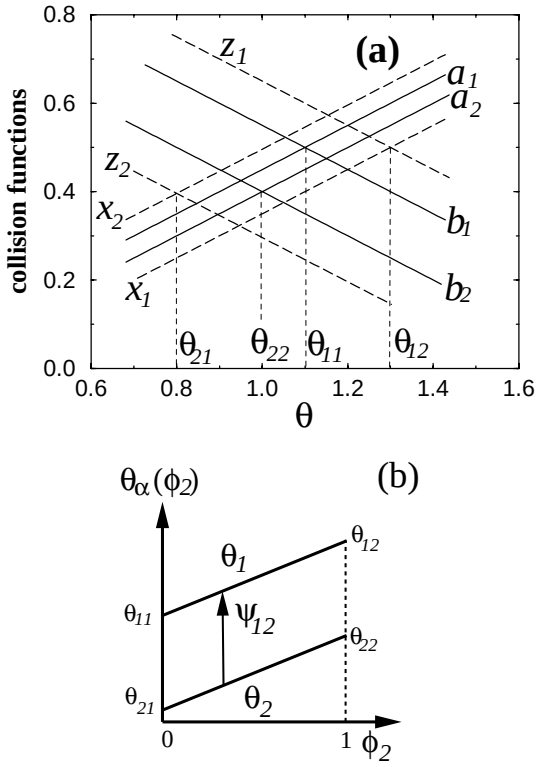

Fig. 5. Case C: mixture of small rough grains (type 1) and large smooth grains (type 2). (a) Collision functions: when the grains differ both in size and in shape, the eight functions are distinct. (b) Generalized angles of repose.

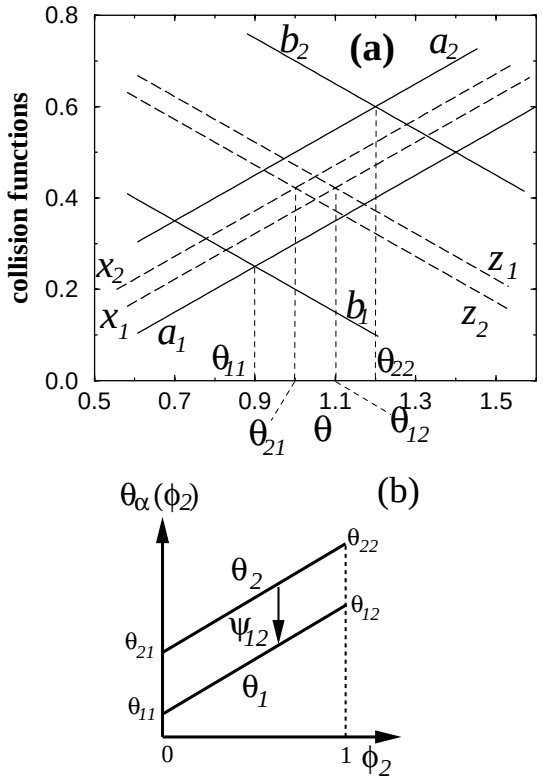

Fig. 6. Case D: mixture of small smooth grains (type 1), and large rough grains (type 2) when the size difference is small. (a) Collision functions. (b) Generalized angles of repose.

However, when the size difference is more important, we obtain a case close to the situation where the particles differ only in their sizes. Then, we have (as postulated in [37])

$$\theta_{21} < \theta_{22} < \theta_{11} < \theta_{12}, \tag{38}$$

and

$$x_1 < a_2 < a_1 < x_2, \qquad z_2 < b_2 < b_1 < z_1. \tag{39}$$

The collision functions and the generalized angles of repose for this case are represented in Figures 5a and 5b.

4.4 Mixture of small smooth grains and large rough grains

We denote "type 1" grains the small smooth grains, and "type 2" the large rough grains ($1 = s = m$ and $2 = l = r$). As explained previously, we have for the different angles of repose

$$\theta_{11} < \theta_{22}, \qquad \theta_{21} < \theta_{12}. \tag{40}$$

We consider here the case when the difference in size is small, and shape segregation effect is more important than size segregation effect. Then in this situation, we have (see Fig. 6b)

$$\theta_{11} < \theta_{21} < \theta_{12} < \theta_{22}. \tag{41}$$

As shown in Figure 6a, the collision functions satisfy

$$a_1 < x_1 < x_2 < a_2, \qquad b_1 < z_2 < z_1 < b_2. \tag{42}$$

5 Segregation in the filling of a silo

5.1 General equations

In order to describe the segregation between the two species predicted by the present model, we study the case of the steady state filling of a two-dimensional silo, which is a simple geometry and has been the focus of experimental studies by different authors [26–29]. Inside a two-dimensional cell made of two vertical plates separated by approximately 0.5 cm, a mixture of two different species is poured with a constant in-going flux. Let us call the horizontal axis the x axis. The cell is located between $0 < x < L$, and the grains are poured at the point of injection at $x = L$ (Fig. 7). We focus on the steady state filling; as the mixture is poured in the cell, the surface of the pile rises uniformly without deforming, at a constant speed w

$$\frac{\partial h}{\partial t} = w. \tag{43}$$

We review some results found for this situation with the minimal model [34]. In the steady state filling, we have

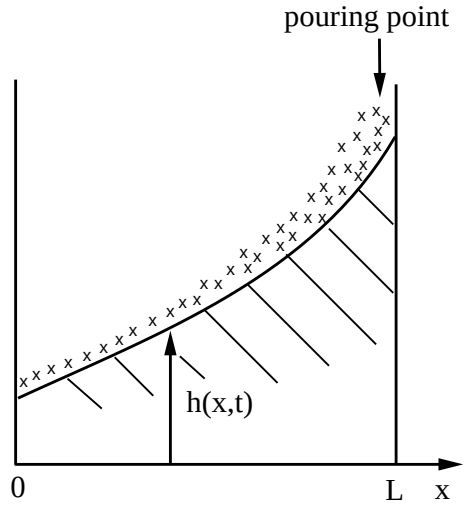

Fig. 7. Filling of a two-dimensional silo, in which a constant flux of grains is poured. In the steady state, the surface of the static grains rises uniformly, at the constant speed w.

$\dot{R}_\alpha = 0$. Then equations (3) and (5), and the boundary condition $R(x = 0) = 0$, imply that the total thickness $R(x)$ of the rolling phase decreases linearly with respect to the distance from the pouring point

$$R(x) = \frac{w}{v}x. \tag{44}$$

The total exchange between the two phases $\dot{R}_1|_{coll} + \dot{R}_2|_{coll}$ can be calculated as a function of the generalized angles of repose, using the collision matrix (20). Then equation (5) yields

$$-w = \gamma[\theta - \theta_1(\phi_2)]R_1 + \gamma[\theta - \theta_2(\phi_1)]R_2. \tag{45}$$

In this expression, the order of magnitude of the right hand side is $\gamma\psi R \sim \psi w x/d$, where $\gamma \simeq v/d$ (Eq. (16)). The ratio of the right hand side of (45) divided by its left hand side is $\sim \psi x/d$. Thus, when $x \gg d/\psi$, the left hand side can be neglected, and we get for the local slope θ

$$\theta = \theta_1(\phi_2)\frac{R_1}{R} + \theta_2(\phi_2)\frac{R_2}{R}\cdot \tag{46}$$

In particular, in the steady state, the value of θ lies between the two generalized angles of repose θ_1 and θ_2. By combining equations (4, 20, 46), we obtain the following expressions of the volume fractions ϕ_α in the static phase

$$\phi_1 = \left(1 + \xi_{12}\frac{R_2}{x_1R_1 + x_2R_2}\right)\frac{R_1}{R},$$
$$\phi_2 = \left(1 - \xi_{12}\frac{R_1}{x_1R_1 + x_2R_2}\right)\frac{R_2}{R}, \tag{47}$$

where

$$\xi_{12} \equiv \gamma\psi_{12} + \Delta x_{12} \tag{48}$$

is a constant in our model. We notice that the minimal model of [34] consists of taking the cross-amplification functions constant independent on the angle, $x_1(\theta) = x_2(\theta) \equiv m$, and $\Delta x_{12} = 0$. With these approximations the minimal model can be solved to obtain a closed form for the concentrations and the rolling grain profiles.

Equations (47) show that segregation happens when rolling grains stop on the static phase; the volume fraction R_α/R of the α grains in the rolling phase is different from the volume fraction ϕ_α of the same species in the static phase. Since the quantity $R_\alpha/(x_1R_1 + x_2R_2)$ is always positive, if $\xi_{12} > 0$ we obtain $\phi_1 > R_1/R$ and $\phi_2 < R_2/R$; type 1 grains are captured more easily than type 2 grains. Conversely, if $\xi_{12} < 0$ we obtain $\phi_1 < R_1/R$ and $\phi_2 > R_2/R$; type 2 grains stop more easily. This behavior induces segregation everywhere in the static phase; the larger $\mid \xi_{12} \mid$ the stronger the segregation.

For instance, let us consider the case where we pour an equal volume mixture, $R_1(x = L) = R_2(x = L)$. If $\xi_{12} > 0$, we obtain at the top of the slope $\phi_1(x = L) > \phi_2(x = L)$. Type 1 rolling grains stop more easily, and the fraction of these grains decrease in the rolling phase ($R_1 < R_2$), while type 2 rolling grains will preferentially stop at the bottom of the slope $\phi_1(x = 0) < \phi_2(x = 0)$. Thus, in this example, the static phase contains mostly type 1 grains in its upper part, and type 2 grains in its lower part.

In the lower part of the pile ($x \ll L$), it is possible to quantify more precisely the segregation for any kind of poured mixture. By doing a linear development of the equations, we can look for a power law behavior valid at the bottom of the slope, as suggested by the solution of the minimal model [34]. If, for instance, we assume ξ_{12} to be positive, we expect that R_1/R tends to zero. We write for $x \ll L$

$$\frac{R_1(x)}{R(x)} \simeq Ax^\eta, \tag{49}$$

where A and η are two positive constants. Then ϕ_1 can be calculated in first order approximation with equations (47)

$$\phi_1(x) \simeq \left(1 + \frac{\xi_{12}}{x_2}\right)Ax^\eta. \tag{50}$$

When we substitute these expressions for R_1/R and ϕ_1 in the relation $\partial R_1/\partial x = w\phi_1/v$ (obtained from Eqs. (4, 5)), we obtain an equation whose compatibility confirms that the type 1 species follows a power-law behavior at the bottom of the slope. This equation also gives the value of the exponent η

$$\eta = \frac{\xi_{12}}{x_2(\theta = \theta_{22})}\cdot \tag{51}$$

Note that the exponent η depends on the granular species. This power law behavior shows that our model predicts continuous segregation; the concentrations of species vary slowly in the container, both types of grains remaining present everywhere. This continuous segregation corresponds to what is observed in experiments, when the two granular species do not have a wide difference in size [29].

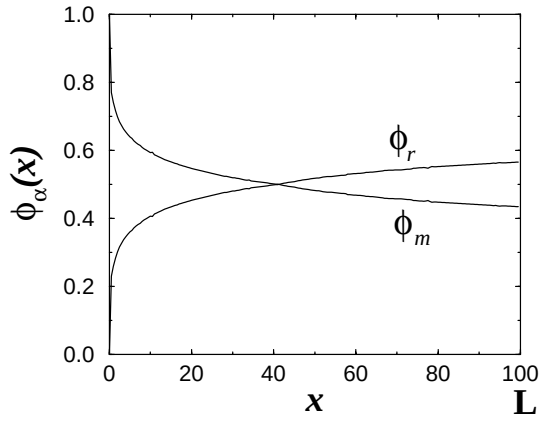

Fig. 8. Case B: grains differing only in their surface properties. Concentration profiles (calculated numerically) during the steady state filling of a silo. The segregation clearly appears at $x = L$, where $R_m = R_r$ but $\phi_m < \phi_r$.

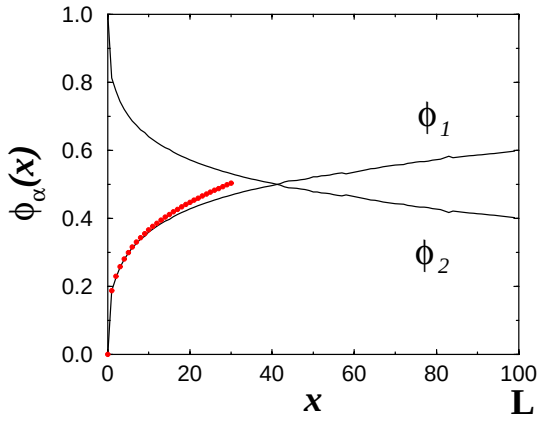

Fig. 9. Case C: small rough grains (type 1) and large smooth grains (type 2). Concentration profiles at the surface calculated numerically in the steady state. The dotted line corresponds to the fit to the analytical expression (50), valid at the bottom of the pile.

5.2 Segregation for the different mixtures

For the different mixtures of grains treated in Section 4, the model predicts continuous segregation during the steady state filling of a silo. In the case of grains differing only in their surface properties, we have $x_r = x_m$ and

$$\xi_{rm} \equiv \gamma\psi_{rm} + \Delta x_{rm} = \gamma\frac{\theta_{rr} - \theta_{mm}}{2} > 0. \qquad (52)$$

The sign of ξ_{rm} indicates that inside the static phase, the rough grains are found preferentially at the top of the silo (see Eq. (47)). In order to quantify more precisely the predictions of the model, we perform a numerical integration of the equations of motion for this case. Figure 8 shows the results calculated in the case of an equal volume mixture of rough grains and smooth grains, $R_r(x = L) = R_m(x = L)$. For this simulation, we chose $\theta_{rr} = 49°$, $\theta_{mm} = 43°$, $\psi_{rm} = 3°$, and $x(\theta = \theta_{rm}) = 0.375\gamma$. Figure 8 shows the volume fractions $\phi_\alpha(x)$ for $0 \leq x \leq L$ in the steady state. Note that segregation clearly appears at $x = L$, where $R_m = R_r$ but $\phi_m < \phi_r$. Figure 8 confirms that our model predicts a continuous segregation, and not a complete one; ϕ_r does not fall suddenly at $x = L/2$, but slowly decreases as x decreases. Similar profiles have been recently obtained with numerical simulations, by using a granular media lattice gas model to study the filling process of a two-dimensional silo with inelastic particles differing in friction coefficients [40].

When the grains differ only in their size, a similar continuous segregation is found, with the smaller grains located preferentially at the top of the pile. Thus our results indicate that the roughest grains or the smallest ones are segregated at the top of the pile, while the largest grains or the smoothest ones are segregated preferentially at the bottom. When we mix grains differing both in size and in surface properties, a competition between size-segregation and shape-segregation appears.

For the mixture treated in Section 4.3 of small rough grains and large smooth grains, the model predicts continuous segregation with the rough and small grains found preferentially at the top of the pile. This is the case of strongest segregation found with the present model, since both size segregation and shape segregation act simultaneously to segregate the small rough grains at the top of the pile and the large smooth grains at the bottom. Figure 9 shows the volume fractions $\phi_\alpha(x)$ calculated numerically when an equal volume mixture of small rough (type 1) grains and large smooth (type 2) grains is poured in the silo. We set $x_0 = 0.4\gamma$, $\Delta x_{12} = -0.13\gamma$, $L = 100$, and use the collision functions shown in Figure 5. Figure 9 shows a continuous segregation which is stronger than in the case of grains differing only in their surface properties (case 4.2, Fig. 8). At the lower end of the slope ($x \ll L$), we have a complete purification of both species due to segregation; $R_1(x)/R$ and $\phi_1(x)$ tend to zero. In that region, we can fit the numerical solution with the analytical expression equation (50) with $\eta = 0.29$.

The last case treated in Section 4 corresponds to a mixture of small smooth grains and large rough grains. The size difference is taken to be small, to allow for the linear development of the collision functions. Thus shape segregation is found to dominate over size segregation, so that the smooth grains are found at the bottom. However, when the effect of size segregation is comparable to the effect of shape segregation, the competition between size and shape segregation gives rise to a different phenomenon. Indeed, experiments show that we obtain either stratification when the large grains are the roughest, or a complete segregation when the large grains are the smoothest [26–29]. The theoretical model proposed in the present article can explain both the complete segregation and the stratification. These phenomena aredue to

the type of segregation that appears directly inside the rolling phase, as explained in the next section.

6 Complete segregation and stratification

So far we have treated the cases when the difference between surface properties and size of the grains is not too wide, hence we could perform linear developments of the collision functions around the region of interest. This situation gives rise to the continuous segregation patterns in all the cases studied in the previous sections. When the difference between the grains size is important, stronger segregation effects are expected. According to experiments [26–29], this occurs when $\rho > 1.5$, where ρ is the ratio of the size of the large grains divided by the size of the small ones. The size segregation is due to segregation at the shear surface between the rolling and the static phase [37], or it may already happen inside the rolling phase [27,39]; small rolling grains tend to fall downward through the gaps in between the large grains, so that they form a sub-layer of small rolling grains underneath the large rolling grains. This phenomenon is called "kinematic sieving", "free-surface segregation" or "percolation" [23,24,27]. The large rolling grains are not in contact with the bulk, and are captured after the small grains. The percolation effect takes place inside the rolling phase if its thickness is larger than (approximately) two or three grain diameters. However, even for a thin flow, strong size segregation occurs in the shear surface between the rolling and static phase if the size difference between the grains is wide enough. In both cases, the large rolling grains are captured only after the small ones, and the collision functions may take the forms proposed in [37] (see Fig. 4 of [38]).

Here we use a suitable modification of the interaction term, in order to take into account the segregation inside the rolling phase within the present formalism. We replace $R_2(x,t)$ in the definition of the interaction term by $R_2(x,t)\exp[-\lambda R_1(x,t)/R(x,t)]$. The exponential factor multiplying $R_2(x,t)$ mimics the fact that the interaction of large rolling grains is screened by the presence of small grains, so that large rolling grains R_2 interact with the grains at the surface of the static phase only when $R_1(x,t) \ll R(x,t)/\lambda$. The dimensionless parameter $\lambda > 0$ measures the degree of percolation [39]. We numerically simulate this model using a mixture of grains differing both in size and shape. When the large grains are smoother than the small grains, we obtain a complete segregation of the mixture (see Fig. 10a). The transition zone between the two species at rest has a size which goes approximately from a few mm to a few cm. When the large grains are rougher than the small grains, Figure 10b shows that we find stratification of the static phase. This stratification results from the competition between size-segregation and shape-segregation. In conclusion, when our model includes the percolation effect, we are able to reproduce the experimental observations obtained with particles of very different sizes [26–29]. Our results are also consistent with the ones found by Makse *et al.* [37–39], to whom we refer for further details.

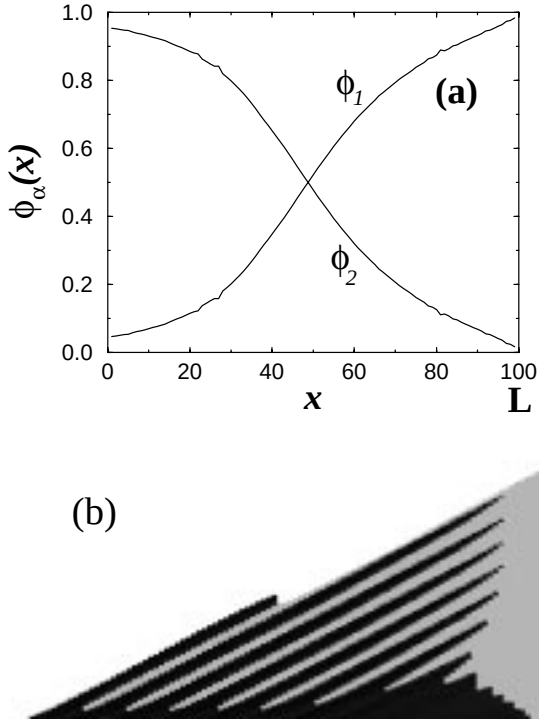

Fig. 10. (a) Concentration profiles obtained numerically showing the complete segregation of a mixture of small rough grains (type 1) and large smooth grains (type 2) when the percolation effect is present. (b) Stratification of a mixture of large rough grains (dark) and small smooth grains (grey), when the percolation effect is included in the model.

7 Discussion

We have proposed an analytical model (called *canonical* model) that explains the continuous segregation observed during the filling of a silo, when the grains have a small difference in size. Our predictions could be precisely tested by experimental measurements. When the two granular species have a wide difference in size, we include, in the canonical model, the percolation effect that appears directly in the rolling phase. The model is then able to reproduce the complete segregation and the stratification observed in experiments; it is also consistent with results recently published by Makse *et al.* who described grains with a wide difference in size.

The canonical model incorporates both differences in size and in surface properties of the grains, and contains several coupling parameters between the two granular species such as the cross-angles of repose, and the two constants x_0 and Δx_{12}. In comparison, the minimal model [34] is simpler than the canonical model since the minimal model contains only one coupling parameter. However, as a consequence, the minimal model cannot take into account a size difference between the particles.

In the present paper, we have applied the canonical model to only one practical situation: the steady state filling of a silo. This situation is interesting, since it has already been described experimentally by different authors. Moreover, the present model for surface flows of granular mixtures could be applied to many different situations. In particular, the segregation that appears during thick avalanches in rotating cylinders could be studied analytically; the results could be compared to the ones published recently for a pure granular species [36,41].

This work has benefited from very stimulating discussions with J.-P. Bouchaud, P. Cizeau, Y. Grasselli, H. J. Herrmann, E. Raphaël, H. E. Stanley, and S. Tomassone. H. Makse thanks BP for financial support.

References

1. R.A. Bagnold, *The Physics of Blown Sand and Desert Dunes* (Chapman and Hall, London, 1941).
2. H.M. Jaeger, S.R. Nagel, Science **255**, 1523 (1992).
3. *Disorder and Granular Media*, edited by D. Bideau, A. Hansen (North-Holland, Amsterdam, 1993).
4. S.F. Edwards, in *Granular Matter: An Interdisciplinary Approach*, edited by A. Mehta (Springer-Verlag, New York, 1994), p. 121.
5. D.E. Wolf, in *Computational Physics: Selected Methods – Simple Exercises – Serious Applications*, edited by K.H. Hoffmann, M. Schreiber (Springer-Verlag, Heidelberg, 1996).
6. H.M. Jaeger, S.R. Nagel, R.P. Behringer, Rev. Mod. Phys. **68**, 1259 (1996).
7. J. Duran, *Sables, Poudres et Grains* (Ed. Eyrolles, 1997, in French).
8. P.-G. de Gennes, in *The Physics of Complex Systems*, edited by F. Mallamace, H.E. Stanley (IOS Press, Amsterdam, 1997).
9. *Physics of Dry Granular Matter*, edited by H.J. Herrmann, J.P. Hovi, S. Luding (Kluwer, Dordrecht, 1998).
10. J.C. Williams, Powder Technol. **15**, 245 (1976).
11. A. Rosato, K.J. Strandburg, F. Prinz, R.H. Swendsen, Phys. Rev. Lett. **58**, 1038 (1987).
12. P. Evesque, J. Rajchenbach, Phys. Rev. Lett. **50**, 44 (1989).
13. J.A.C. Gallas, H.J. Herrmann, S. Sokolowski, Phys. Rev. Lett. **69**, 1371 (1992).
14. J.B. Knight, H.M. Jaeger, S.R. Nagel, Phys. Rev. Lett. **70**, 3728 (1993).
15. O. Zik, D. Levine, S.G. Lipson, S. Shtrikman, J. Stavans, Phys. Rev. Lett. **73**, 644 (1994).
16. K.M. Hill, J. Kakalios, Phys. Rev. E **49**, R3610 (1994).
17. W. Cooke, S. Warr, J.M. Huntley, R.C. Ball, Phys. Rev. E **53**, 2812 (1996).
18. E. Clément, J. Rajchenbach, J. Duran, Europhys. Lett. **30**, 7 (1995).
19. F. Cantelaube, D. Bideau, Europhys. Lett. **30**, 133 (1995).
20. R.L. Brown, J. Inst. Fuel **13**, 15 (1939).
21. R.A. Bagnold, Proc. R. Soc. London A **225**, 49 (1954).
22. J.C. Williams, Univ. Sheffield Fuel Soc. J. **14**, 29 (1963).
23. J.A. Drahun, J. Bridgwater, Powder Technol. **36**, 39 (1983).
24. S. Savage, C.K.K. Lun, J. Fluid Mech. **189**, 311 (1988).
25. P. Meakin, Physica A **163**, 733 (1990).
26. H.A. Makse, S. Havlin, P.R. King, H.E. Stanley, Nature **386**, 379 (1997).
27. H.A. Makse, R.C. Ball, H.E. Stanley, S. Warr, Phys. Rev. E **58**, 3357 (1998).
28. J. Koeppe, M. Enz, J. Kakalios, in *Powders and Grains 97*, edited by R. Behringer, J. Jenkins (Balkena, Rotterdam, 1997), p. 443.
29. Y. Grasselli, H.J. Herrmann, Granular Matter J. **1**, 43 (1998).
30. J.-P. Bouchaud, M.E. Cates, J.R. Prakash, S.F. Edwards, Phys. Rev. Lett. **74**, 1982 (1995).
31. J.-P. Bouchaud, M.E. Cates, J.R. Prakash, S.F. Edwards, J. Phys. I France **4**, 1383 (1994).
32. A. Mehta in *Granular Matter: An Interdisciplinary Approach*, edited by A. Mehta (Springer-Verlag, New York, 1994).
33. P.-G. de Gennes, C. R. Acad. Sci. (Paris) IIb **321**, 501 (1995).
34. T. Boutreux, P.-G. de Gennes, J. Phys. I France **6**, 1295 (1996).
35. T. Boutreux, Eur. Phys. J. B **6**, 419 (1998).
36. T. Boutreux, Ph.D. thesis, University of Paris VI, 1998.
37. H.A. Makse, P. Cizeau, H.E. Stanley, Phys. Rev. Lett. **78**, 3298 (1997).
38. H.A. Makse, Phys. Rev. E **56**, 7008 (1997).
39. P. Cizeau, H.A. Makse, H.E. Stanley, Phys. Rev. E. **59**, 4408 (1999)
40. A. Károlyi, J. Kertész, S. Havlin, H.A. Makse, H.E. Stanley, Europhys. Lett. **44**, 388 (1998).
41. T. Boutreux, E. Raphaël, P.-G. de Gennes, Phys. Rev. E **58**, 4692 (1998).